Chapter 5

TWO-MAGNON BOUND STATES IN FERROMAGNETS

5.1. Two-Spin Deviation Eigenstates

In Chapter 1, we have seen how to build the excited states of a ferromagnet by adding one or two spin deviations. We have shown that a state with one spin deviation delocalized over the whole lattice (spin wave) is an eigenstate of the Heisenberg Hamiltonian. On the contrary, the state with two spin deviations delocalized over the lattice (two "free" spin waves) is not an eigenstate of the Heisenberg Hamiltonian: Only in the thermodynamic limit, the two "interacting" spin waves become asymptotically free if their energy is inside the two-magnon band. Moreover, in Chapter 4, we have shown that the poles of the T-matrix correspond to the bound states of the system. In this chapter, we will obtain the two-magnon bound states starting directly from the boson operators corresponding to the creation and destruction operators of magnons. This procedure[38] is the most direct way to arrive at the two-magnon bound state of a ferromagnet.

Consider the state made up of a linear combination of states with two magnons of momenta $\boldsymbol{k}_1 = \frac{1}{2}\boldsymbol{K} + \boldsymbol{q}$ and $\boldsymbol{k}_2 = \frac{1}{2}\boldsymbol{K} - \boldsymbol{q}$

$$|\boldsymbol{K}\rangle = \sum_{\boldsymbol{q}} f_{\boldsymbol{K}}(\boldsymbol{q})\ a^{+}_{\frac{1}{2}\boldsymbol{K}+\boldsymbol{q}} a^{+}_{\frac{1}{2}\boldsymbol{K}-\boldsymbol{q}}|0\rangle, \tag{5.1.1}$$

where $f_{\boldsymbol{K}}(\boldsymbol{q})$ are coefficients to be determined in such a way that the state (5.1.1) is eigenstate of the Heisenberg Hamiltonian realized in terms of Bose operators using the DM transformation as given by Eqs. (4.1.3)–(4.1.5a). Imposing that $\mathcal{H}|\boldsymbol{K}\rangle = E|\boldsymbol{K}\rangle$ and defining $\hbar\omega = E - E_{\rm GS}$ where $E_{\rm GS}$ is the ground-state energy of the ferromagnet, one obtains

$$\begin{aligned}(\hbar\omega - \hbar\omega_{\frac{1}{2}\boldsymbol{K}+\boldsymbol{q}} - \hbar\omega_{\frac{1}{2}\boldsymbol{K}-\boldsymbol{q}}) f_{\boldsymbol{K}}(\boldsymbol{q}) \\ = \frac{zJ}{N}\sum_{\boldsymbol{q}'}(\gamma_{\frac{1}{2}\boldsymbol{K}+\boldsymbol{q}} + \gamma_{\frac{1}{2}\boldsymbol{K}-\boldsymbol{q}} - \gamma_{\boldsymbol{q}+\boldsymbol{q}'} - \gamma_{\boldsymbol{q}-\boldsymbol{q}'}) f_{\boldsymbol{K}}(\boldsymbol{q}').\end{aligned} \tag{5.1.2}$$

Equation (5.1.2) illustrates clearly that the state with two free spin waves (left-hand side) is never the eigenstate of the boson Hamiltonian because of the presence of

the right-hand side coming from the interaction potential between the spin waves. Using the definition $\gamma_{\boldsymbol{q}} = \frac{1}{z}\sum_{\boldsymbol{\delta}} e^{i\boldsymbol{q}\cdot\boldsymbol{\delta}}$, Eq. (5.1.2) becomes

$$\left[\hbar\omega - 4JS\sum_{\boldsymbol{\delta}}\left(1-\cos\frac{\boldsymbol{K}}{2}\cdot\boldsymbol{\delta}\ \cos\boldsymbol{q}\cdot\boldsymbol{\delta}\right)\right] f_{\boldsymbol{K}}(\boldsymbol{q}) = \frac{2J}{N}\sum_{\boldsymbol{\delta}}\cos\boldsymbol{q}\cdot\boldsymbol{\delta}\sum_{\boldsymbol{q}'}\left(\cos\frac{\boldsymbol{K}}{2}\cdot\boldsymbol{\delta}-\cos\boldsymbol{q}'\cdot\boldsymbol{\delta}\right) f_{\boldsymbol{K}}(\boldsymbol{q}') \tag{5.1.3}$$

which coincides with Eq. (1.4.13). As we have shown in Chapter 1, the two-spin wave bound states are determined as the solutions of the Eq. (1.4.30) that is

$$\det\left[\mathbf{1}-\frac{1}{2S}\mathbf{B}(\boldsymbol{K},\omega)\right]=0. \tag{5.1.4}$$

For cubic lattices (LC, SQ, SC), defining $\alpha,\beta = x,y,z$ one has

$$B_{\alpha\beta}(\boldsymbol{K},\omega) = \frac{8JS}{N}\sum_{\boldsymbol{q}}\frac{\cos q_\alpha\left(\cos K_\beta/2-\cos q_\beta\right)}{\hbar\omega-\hbar\omega_{\boldsymbol{K}}(\boldsymbol{q})} \tag{5.1.5}$$

and

$$f_{\boldsymbol{K}}(\boldsymbol{q}) = \frac{4J}{N}\sum_{\alpha}\frac{\cos q_\alpha}{\hbar\omega-\hbar\omega_{\boldsymbol{K}}(\boldsymbol{q})}G^\alpha_{\boldsymbol{K}}, \tag{5.1.6}$$

where $G^\alpha_{\boldsymbol{K}}$ are obtained from the system

$$\begin{pmatrix} 1-\frac{1}{2S}B_{xx} & -\frac{1}{2S}B_{xy} & -\frac{1}{2S}B_{xz} \\ -\frac{1}{2S}B_{yx} & 1-\frac{1}{2S}B_{yy} & -\frac{1}{2S}B_{yz} \\ -\frac{1}{2S}B_{zx} & -\frac{1}{2S}B_{zy} & 1-\frac{1}{2S}B_{zz} \end{pmatrix}\begin{pmatrix} G^x_{\boldsymbol{K}} \\ G^y_{\boldsymbol{K}} \\ G^z_{\boldsymbol{K}} \end{pmatrix} = 0. \tag{5.1.7}$$

In 2D (SQ lattice) and in 1D (LC), Eq. (5.1.7) reduces to a 2×2 matrix equation and a scalar equation, respectively.

5.2. Bound States in 1D

Let us begin considering the LC for which Eq. (5.1.7) reduces to the scalar equation

$$\left[1-\frac{1}{2S\pi}\int_0^\pi dq\ \frac{\cos q\left(\cos\frac{K}{2}-\cos q\right)}{x+\cos\frac{K}{2}\cos q}\right] G_K = 0 \tag{5.2.1}$$

where $x = \frac{\hbar\omega}{8JS}-1$. The amplitude of the wave function is given by

$$f_K(q) = \frac{\cos q}{2S\left(x+\cos\frac{K}{2}\cos q\right)}G_K, \tag{5.2.2}$$

where G_K is an arbitrary constant to be fixed by the normalization of the wave function. The integral appearing in Eq. (5.2.1) is evaluated[3] as "principal part" and it gives different contributions accordingly if x is lesser than $-\cos\frac{K}{2}$ or greater

than $\cos\frac{K}{2}$. Consequently, two scalar equations are obtained for the bound states in 1D: for $-1 < x < -\cos\frac{K}{2}$, corresponding to an energy below the bottom of the two-spin wave band, that is $0 < \hbar\omega < \hbar\omega_{\rm bottom} = 8JS(1-\cos\frac{K}{2})$, one has

$$1-\frac{1}{2S}\left(1+\frac{x}{\cos^2\frac{K}{2}}\right)\left(1+\frac{x}{\sqrt{x^2-\cos^2\frac{K}{2}}}\right)=0, \tag{5.2.3}$$

while for $x > \cos\frac{K}{2}$, corresponding to an energy above the top of the two-spin wave band, that is $\hbar\omega > \hbar\omega_{\rm top} = 8JS(1+\cos\frac{K}{2})$, one has

$$1-\frac{1}{2S}\left(1+\frac{x}{\cos^2\frac{K}{2}}\right)\left(1-\frac{x}{\sqrt{x^2-\cos^2\frac{K}{2}}}\right)=0. \tag{5.2.4}$$

Equation (5.2.3) has always at least one root since its left-hand side is $[2S+(2S-1)\sin\frac{K}{2}]/[2S(1+\sin\frac{K}{2})] > 0$ for $x=-1$ and goes to $-\infty$ for $x \to -\cos\frac{K}{2}$ crossing the x-axis in one point $x_{\rm BS}$ such that $-1 < x_{\rm BS} < -\cos\frac{K}{2}$. On the contrary, Eq. (5.2.4) has no solution since its left-hand side is a positive monotonic decreasing function from $+\infty$ for $x \to \cos\frac{K}{2}$ to 1 for $x \to \infty$. Indeed, it is direct to prove that the first derivative with respect to x of the left-hand side of Eq. (5.2.4) is negative for any $x > \cos\frac{K}{2}$. Then in 1D, only one two-magnon bound state exists for any wavevector K below the two-magnon band. To obtain explicitly the energy of this bound state, we look for the solution of Eq. (5.2.3) for a generic K and S. The most direct way is to square Eq. (5.2.3) that leads to the cubic equation

$$4Sx^3+\left[1-4S(S-1)\cos^2\frac{K}{2}\right]x^2-2(2S-1)x\cos^2\frac{K}{2}+(2S-1)^2\cos^4\frac{K}{2}=0. \tag{5.2.5}$$

Equation (5.2.5) has only one root that satisfies the condition $-1 < x < -\cos\frac{K}{2}$ as required by the original Eq. (5.2.3). Indeed, for $S < 3$, Eq. (5.2.5) has one real root and a pair of complex conjugate roots. For $S \geq 3$, Eq. (5.2.5) has three real roots for $K < K_c(S)$ and one real root and a pair of complex conjugate roots for $K > K_c(S)$ where $K_c(S)$ is given by 0.19781π, $0.46624\pi, 0.58283\pi, 0.65488\pi, 0.70483\pi, \ldots$ for $S = 3, \frac{7}{2}, 4, \frac{9}{2}, 5, \ldots$, respectively. In any case, these real roots are always positive and do not satisfy the condition $-1 < x < -\cos\frac{K}{2}$, so that they have to be rejected. Note that at the ZB ($K=\pi$), one obtains $x_{\rm BS} = -\frac{1}{4S}$, corresponding to an energy $\hbar\omega_{\rm BS} = 8JS(1-\frac{1}{4S})$ and showing that the bound state disappears in the classical limit $S \to \infty$. For $S = \frac{1}{2}$, the solution of Eq. (5.2.3) or (5.2.5) can be given in analytic form leading to

$$\hbar\omega(K) = 2J\sin^2\frac{K}{2}. \tag{5.2.6}$$

In Fig. 5.1, the two-magnon bound state energy in units of $8JS$ for a LC is shown as function of the reduced wavevector K/π for several values of the spin S. The light dashed lines represent the bottom and the top of the two-magnon band. The continuous and dotted curves represent the energy of the two-magnon bound state

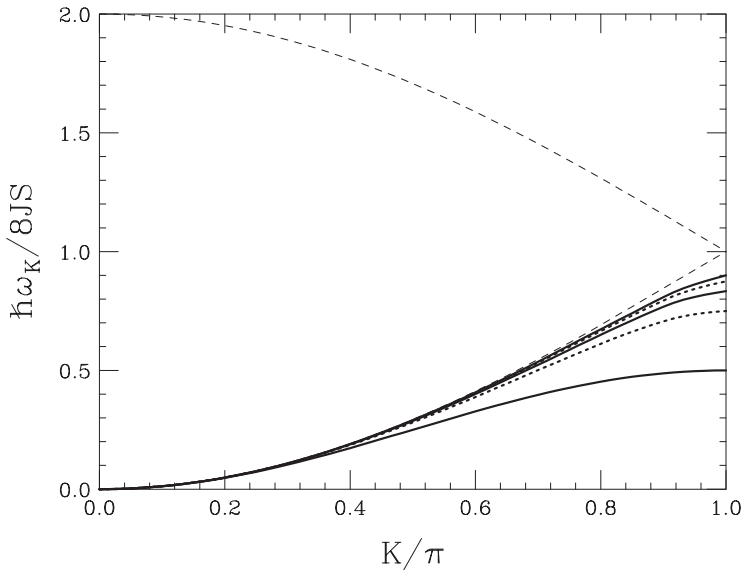

Fig. 5.1. Two-magnon bound state energy versus wavevector for the LC and several values of the spin (alternation of continuous and dotted curves). Going from the lowest to the highest curve the spin assumes the values $S = \frac{1}{2}, 1, \frac{3}{2}, 2, \frac{5}{2}$. The light dashed lines represent the bottom and the top of the two-magnon band.

for $S = \frac{1}{2}, 1, \frac{3}{2}, 2, \frac{5}{2}$ moving from the bottom to the top. In order to prove that the bound state energy is always below the bottom of the two-magnon band, we expand both the energy of the bottom of the two-magnon band and the bound state energy for $K \to 0$. From the expansion of the energy of the bottom of the two-magnon band in powers of K^2, we obtain

$$\frac{\hbar\omega_{\rm bottom}}{8JS} = \frac{K^2}{8} - \frac{K^4}{384} + \frac{K^6}{46080} + \cdots . \tag{5.2.7}$$

Using Eq. (5.2.5) and assuming that $x = -1 + AK^2 + B(S)K^4 + C(S)K^6 + \cdots$, we obtain a polynomial in K^2: imposing that the coefficients of such polynomial are zero we obtain

$$A = \frac{1}{8}, \quad B = -\frac{3 + 4S^2}{1536S^2}, \quad C = -\frac{45 - 180S + 120S^2 - 16S^4}{737280S^4}. \tag{5.2.8}$$

The difference between the energy of the bottom of the two-magnon band and the energy of the bound state in units of $8JS$ is

$$\Delta(S) = \frac{\hbar\left(\omega_{\rm bottom} - \omega_{\rm BS}\right)}{8JS} = \frac{K^4}{512S^2} + \frac{\left(3 - 12S + 8S^2\right)K^6}{49152S^4}. \tag{5.2.9}$$

As one can see from Eq. (5.2.9), the difference $\Delta(S)$ is positive for any S for $K \to 0$, so that the bound state energy is below the two-magnon band for any wavevector $K \neq 0$.

The eigenstate belonging to the eigenvalue $\hbar\omega_{\rm BS}$ is given by Eqs. (5.1.1) and (5.2.2)

$$|K\rangle = \frac{G_K}{2S}\sum_q \frac{\cos q}{x_{\rm BS}+\cos\frac{K}{2}\cos q} a^+_{\frac{K}{2}+q}a^+_{\frac{K}{2}-q}|0\rangle. \tag{5.2.10}$$

It is interesting to write the eigenstate $|K\rangle$ in terms of localized spin deviations using the Fourier transform given by Eq. (2.2.14): one has

$$|K\rangle = \frac{G_K}{2S}\sum_{l,m} e^{i\frac{K}{2}(l+m)}\frac{1}{N}\sum_q e^{iq(l-m)}\frac{\cos q}{x_{\rm BS}+\cos\frac{K}{2}\cos q} a^+_l a^+_m|0\rangle. \tag{5.2.11}$$

In the thermodynamic limit, the sum over q in Eq. (5.2.11) can be transformed into an integral like

$$\frac{1}{\pi}\int_0^\pi dq \frac{\cos[q(l-m)]\cos q}{x_{\rm BS}+\cos\frac{K}{2}\cos q} = \frac{1}{\cos\frac{K}{2}}[\delta_{l,m}-I_K(l-m)] \tag{5.2.12}$$

where[3]

$$\begin{aligned} I_K(n) &= \frac{1}{\pi}\int_0^\pi dq \frac{\cos nq}{1+\frac{\cos\frac{K}{2}}{x_{\rm BS}}\cos q} \\ &= \frac{|x_{\rm BS}|}{\sqrt{x^2_{\rm BS}-\cos^2\frac{K}{2}}}\left[\frac{|x_{\rm BS}|-\sqrt{x^2_{\rm BS}-\cos^2\frac{K}{2}}}{\cos\frac{K}{2}}\right]^{|n|} \\ &= \frac{|x_{\rm BS}|}{\sqrt{x^2_{\rm BS}-\cos^2\frac{K}{2}}}e^{-\frac{|n|}{\xi}} \end{aligned} \tag{5.2.13}$$

with

$$\xi = \frac{1}{\ln\left(\frac{\cos\frac{K}{2}}{|x_{\rm BS}|-\sqrt{x^2_{\rm BS}-\cos^2\frac{K}{2}}}\right)}. \tag{5.2.14}$$

Replacing Eq. (5.2.13) into Eq. (5.2.11), one obtains

$$|K\rangle = \frac{G_K}{2S}\sum_{l,m} e^{i\frac{K}{2}(l+m)}\frac{1}{\cos\frac{K}{2}}\left[\delta_{l,m}-\frac{|x_{\rm BS}|}{\sqrt{x^2_{\rm BS}-\cos^2\frac{K}{2}}}e^{-\frac{|l-m|}{\xi}}\right]a^+_l a^+_m|0\rangle \tag{5.2.15}$$

that is an exponential decay of the wave function with the distance between the two localized deviations. This means that only states with two deviations close to each other contribute significantly to the bound state wave function.

For $S = 1/2$, the analytic solution $x_{\rm BS} = -\frac{1}{2}(1+\cos^2\frac{K}{2})$ was obtained in Eq. (5.2.6). Replacing such result in Eq. (5.2.15) and noticing that $(a^+_l)^2|0\rangle = 0$ the

eigenstate of the bound state becomes

$$|K\rangle = -G_K \sum_{l\neq m} e^{i\frac{K}{2}(l+m)} \frac{1}{\cos\frac{K}{2}} \frac{3+\cos K}{1-\cos K} e^{-\frac{|l-m|}{\xi}} a_l^+ a_m^+ |0\rangle, \tag{5.2.16}$$

where

$$\xi = \frac{1}{\ln\left(\frac{1}{\cos\frac{K}{2}}\right)}. \tag{5.2.17}$$

Equation (5.2.16) looks very similar to Eq. (2.22) of Oguchi.[38] The light discrepancy comes from the way of computing the integral (5.2.13). Indeed, in the paper of Oguchi,[38] the integral (5.2.13) was evaluated by changing the upper limit of integration from π to ∞ since the author was interested in the behaviour of the amplitude of the eigenstate for large $|l-m|$. This approximation does not change the qualitative conclusion about the exponential decay of the amplitude but slightly changes the quantitative result. Note that for $K \to 0$, the correlation length goes to infinity, so that the decay of the amplitude with the distance is very slow and the two deviations may be located at an arbitrary distance. On the contrary, for $K = \pi$, the correlation length goes to zero implying that the two deviations are located on NN sites. Going from for $K = 0$ to $K = \pi$, the correlation length decays monotonically from ∞ to 0.

5.3. Bound States in 2D

In a SQ lattice, the bound states are obtained as solutions of Eq. (5.1.4) for which

$$\begin{aligned} B_{xx}(\boldsymbol{K},\omega) &= \frac{1}{\pi^2}\int_0^\pi dq_x \int_0^\pi dq_y \frac{\cos q_x\left(\cos\frac{K_x}{2} - \cos q_x\right)}{x + \cos\frac{K_x}{2}\cos q_x + \cos\frac{K_y}{2}\cos q_y} \\ &= \mp\frac{1}{\pi}\int_0^\pi dq \frac{\cos q\left(\cos\frac{K_x}{2} - \cos q\right)}{\sqrt{\left(x+\cos\frac{K_x}{2}\cos q\right)^2 - \cos^2\frac{K_y}{2}}}, \end{aligned} \tag{5.3.1}$$

$$\begin{aligned} B_{xy}(\boldsymbol{K},\omega) &= \frac{1}{\pi^2}\int_0^\pi dq_x \int_0^\pi dq_y \frac{\cos q_x\left(\cos\frac{K_y}{2} - \cos q_y\right)}{x + \cos\frac{K_x}{2}\cos q_x + \cos\frac{K_y}{2}\cos q_y} \\ &= \frac{\cos\frac{K_y}{2}}{\cos\frac{K_x}{2}} \pm \frac{1}{\cos\frac{K_x}{2}}\frac{1}{\pi}\int_0^\pi dq \frac{\left(x+\cos\frac{K_y}{2}\cos q\right)\left(\cos\frac{K_y}{2} - \cos q\right)}{\sqrt{\left(x+\cos\frac{K_y}{2}\cos q\right)^2 - \cos^2\frac{K_x}{2}}}, \end{aligned} \tag{5.3.2}$$

$$\begin{aligned} B_{yx}(\boldsymbol{K},\omega) &= \frac{1}{\pi^2}\int_0^\pi dq_x \int_0^\pi dq_y \frac{\cos q_y\left(\cos\frac{K_x}{2} - \cos q_x\right)}{x + \cos\frac{K_x}{2}\cos q_x + \cos\frac{K_y}{2}\cos q_y} \\ &= \frac{\cos\frac{K_x}{2}}{\cos\frac{K_y}{2}} \pm \frac{1}{\cos\frac{K_y}{2}}\frac{1}{\pi}\int_0^\pi dq \frac{\left(x+\cos\frac{K_x}{2}\cos q\right)\left(\cos\frac{K_x}{2} - \cos q\right)}{\sqrt{\left(x+\cos\frac{K_x}{2}\cos q\right)^2 - \cos^2\frac{K_y}{2}}}, \end{aligned} \tag{5.3.3}$$

$$B_{yy}(\boldsymbol{K},\omega)=\frac{1}{\pi^2}\int_0^\pi dq_x\int_0^\pi dq_y\frac{\cos q_y\big(\cos\frac{K_y}{2}-\cos q_y\big)}{x+\cos\frac{K_x}{2}\cos q_x+\cos\frac{K_y}{2}\cos q_y}$$

$$=\mp\frac{1}{\pi}\int_0^\pi dq\frac{\cos q\big(\cos\frac{K_y}{2}-\cos q\big)}{\sqrt{\big(x+\cos\frac{K_y}{2}\cos q\big)^2-\cos^2\frac{K_x}{2}}}, \tag{5.3.4}$$

where the upper sign has to be assumed for $-2<x<-\cos\frac{K_x}{2}-\cos\frac{K_y}{2}$, corresponding to energies below the two-magnon band and the lower sign has to be assumed for $x>\cos\frac{K_x}{2}+\cos\frac{K_y}{2}$, corresponding to energies above the two-magnon band. Remember that $x=\frac{\hbar\omega}{8JS}-2$. One integration in Eqs. (5.3.1)–(5.3.4) has been performed taking advantage from the relationship[3]

$$\frac{1}{\pi}\int_0^\pi d\xi\frac{1}{a+\cos\xi}=\pm\frac{1}{\sqrt{a^2-1}} \tag{5.3.5}$$

for $a>1$ (upper sign) and $a<-1$ (lower sign), respectively. The integrals (5.3.1)–(5.3.4) may be expressed in terms of elliptic integrals,[39] however, because of the complexity of the final formula we choose to perform the last integration numerically. It should be noted that for a general point in the BZ, the integrals (5.3.1)–(5.3.4) are all distinct and the equation for the bound states (5.1.4) writes

$$\left(1-\frac{B_{xx}}{2S}\right)\left(1-\frac{B_{yy}}{2S}\right)-\frac{B_{xy}\,B_{yx}}{4S^2}=0. \tag{5.3.6}$$

To check the reliability of the numerical calculation we focus on some points of the BZ for which integrals (5.3.1)–(5.3.4) can be written in a simple analytic form. For $\boldsymbol{K}=(\pi,\pi)$, for instance, one has $B_{xx}=B_{yy}=-\frac{1}{2x}$ and $B_{xy}=B_{yx}=0$ so that Eq. (5.3.6) becomes

$$\left(1+\frac{1}{4Sx}\right)^2=0. \tag{5.3.7}$$

Equation (5.3.7) implies that at the ZC two degenerate bound states exist with energy

$$\hbar\omega_{\rm BS}(\pi,\pi)=16JS\left(1-\frac{1}{8S}\right). \tag{5.3.8}$$

Along the line (K,π), Eqs. (5.3.1)–(5.3.4) reduce to

$$B_{xx}=\frac{1}{\pi}\int_0^\pi dq\frac{\cos q\,\big(\cos\frac{K}{2}-\cos q\big)}{x+\cos\frac{K}{2}\cos q}=\left(1+\frac{x}{\cos^2\frac{K}{2}}\right)\left(1\pm\frac{x}{\sqrt{x^2-\cos^2\frac{K}{2}}}\right), \tag{5.3.9}$$

$$B_{yy}=-\frac{1}{2\pi}\int_0^\pi dq\frac{1}{x+\cos\frac{K}{2}\cos q}=\pm\frac{1}{2}\frac{1}{\sqrt{x^2-\cos^2\frac{K}{2}}} \tag{5.3.10}$$

and $B_{xy} = B_{yx} = 0$. The bound state equation (5.3.6) splits into the couple of equations

$$1 - \frac{1}{2S}\left(1 + \frac{x}{\cos^2\frac{K}{2}}\right)\left(1 \pm \frac{x}{\sqrt{x^2 - \cos^2\frac{K}{2}}}\right) = 0 \tag{5.3.11}$$

and

$$1 \mp \frac{1}{4S}\,\frac{1}{\sqrt{x^2 - \cos^2\frac{K}{2}}} = 0. \tag{5.3.12}$$

Equation (5.3.11) coincides with Eqs. (5.2.3) and (5.2.4), so that we conclude that only one solution exists for $-1 < x < -\cos\frac{K}{2}$ and no solution exists for $x > \cos\frac{K}{2}$. For $S = 1/2$, the solution of Eq. (5.3.11) (upper sign) is $x_{\rm BS} = -\frac{1}{2}(1 + \cos^2\frac{K}{2})$ leading to the bound state energy

$$\hbar\omega^{(1)}_{\rm BS}(K,\pi) = 2J\left(3 - \cos^2\frac{K}{2}\right). \tag{5.3.13}$$

Another bound state is obtained from Eq. (5.3.12) by choosing the upper sign while no solution is obtained by the same equation by choosing the lower sign. The energy of this second bound state is given by

$$\hbar\omega^{(2)}_{\rm BS}(K,\pi) = 16JS\left(1 - \frac{1}{2}\sqrt{\frac{1}{16S^2} + \cos^2\frac{K}{2}}\right). \tag{5.3.14}$$

From Eqs. (5.3.11) and (5.3.12), one sees that two bound states exist for any wavevector $\boldsymbol{K} = (K,\pi)$ below the two-magnon band. The same conclusion holds for $\boldsymbol{K} = (\pi, K)$. The two-magnon bound states of wavevector $\boldsymbol{K} = (\pi, K)$ are shown in the central panel of Fig. 5.2. The light dashed lines represent the top and bottom of the two-magnon band.

Now, we look for the bound states for $\boldsymbol{K} = (K, 0)$. In this case, the integrals (5.3.1)–(5.3.4) are evaluated numerically and the zeros of Eq. (5.3.6) are obtained. Only the choice of the upper sign leads to a solution so that one can conclude that the existence of the bound states is limited to the energy region below the two-magnon band. In the right panel of Fig. 5.2, one can see that only one bound state is found for $\boldsymbol{K} = (K, 0)$ and the same result is obtained for $\boldsymbol{K} = (0, K)$. The bound state energy differs from the bottom of the two-magnon band of less than $16JS \times 10^{-7}$ for $K < 0.7\pi$. This is the reason why the bound state appears indistinguishable from the bottom of the two-magnon band in the right panel of Fig. 5.2. To check that the bound state is really below the bottom of the two-magnon band for any K, we try to evaluate analytically the difference between the bottom of the two-magnon band and the bound state energy. To do this, assume $x_{\rm BS} = -1 - \cos\frac{K}{2} - \epsilon$ which leads to a bound state energy $\hbar\omega_{\rm BS} = \hbar\omega_{\rm bottom} - 8JS\epsilon$. Putting this value of $x_{\rm BS}$ into Eqs. (5.3.1)–(5.3.4), in the limit $\epsilon \to 0$ we obtain

$$B_{xx} = -\frac{1 - \cos\frac{K}{2}}{2\pi\sqrt{\cos\frac{K}{2}}}\ln\epsilon + B^{\rm reg}_{xx}, \tag{5.3.15}$$

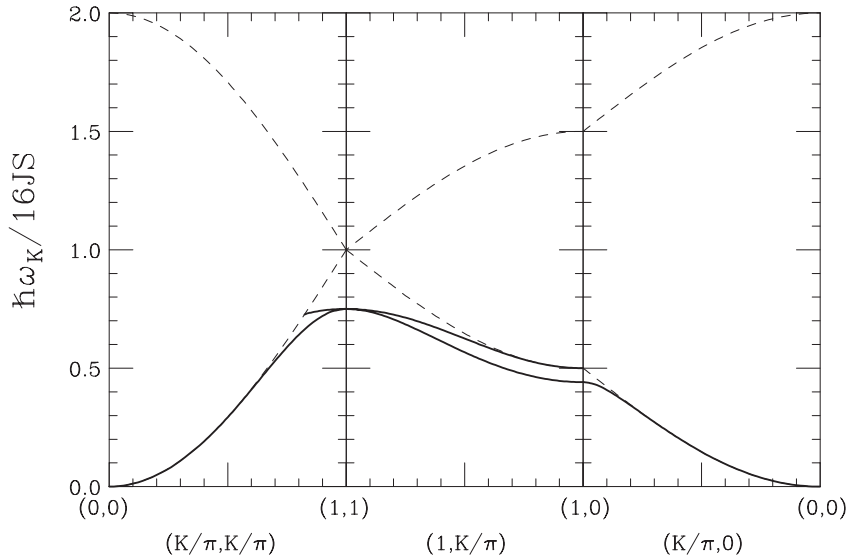

Fig. 5.2. Two-magnon bound state energy versus wavevector along three high symmetry directions (K,K), (π,K) and $(K,0)$ for a SQ lattice with $S=1/2$. The light dashed lines represent the top and the bottom of the two-magnon band. The continuous heavy curves represent the bound states.

where

$$B_{xx}^{\rm reg} = -\frac{1}{\pi\sqrt{\cos\frac{K}{2}}}\int_0^\pi dq \frac{\cos q\sqrt{1-\cos q}}{\sqrt{2+\cos\frac{K}{2}\,(1-\cos q)}} + \frac{1-\cos\frac{K}{2}}{\pi\sqrt{\cos\frac{K}{2}}}\ln\left(\pi\sqrt{2\cos\frac{K}{2}}\right)$$
$$+\frac{1-\cos\frac{K}{2}}{\pi\sqrt{\cos\frac{K}{2}}}\int_0^\pi dq\left\{\frac{\cos q}{\sqrt{(1-\cos q)\left[2+\cos\frac{K}{2}\,(1-\cos q)\right]}}-\frac{1}{q}\right\}. \quad (5.3.16)$$

As one can see from Eq. (5.3.15), B_{xx} diverges logarithmically when the energy of the bound state meets the energy of the bottom of the two-magnon band. This divergence is due to the fact that the integrand diverges as $\frac{1}{q}$ for $q\to 0$. The "regular" contribution given by Eq. (5.3.16) is obtained by subtracting the divergent contribution (first term of the series expansion in q of the integrand) and evaluating the difference for $\epsilon=0$. This approach leads to the third term of Eq. (5.3.16). The "singular" part is then obtained by evaluating directly the integral of the term subtracted for $\epsilon\neq 0$. The second term of Eq. (5.3.16) comes from the integral of the singular part evaluated at $q=\pi$ and taking the limit $\epsilon\to 0$. The above procedure is not required to evaluate B_{xy} because it remains finite for $\epsilon=0$ since the vanishing of the denominator for $q\to 0$ is compensated by a concomitant vanishing of the numerator. The result is

$$B_{xy} = \frac{1}{\cos\frac{K}{2}}\left[1-\frac{1}{\pi}\int_0^\pi dq\frac{\left(1+\cos\frac{K}{2}-\cos q\right)\sqrt{1-\cos q}}{\sqrt{2\cos\frac{K}{2}+1-\cos q}}\right]. \quad (5.3.17)$$

To evaluate B_{yx} the same procedure used for B_{xx} is necessary and one obtains

$$B_{yx} = -\frac{1-\cos\frac{K}{2}}{2\pi\sqrt{\cos\frac{K}{2}}}\ln\epsilon + B_{yx}^{\rm reg}, \tag{5.3.18}$$

where

$$\begin{aligned} B_{yx}^{\rm reg} = &-\frac{1}{\pi\sqrt{\cos\frac{K}{2}}}\int_0^\pi dq \frac{\left[1+\cos\frac{K}{2}\,(1-\cos q)\right]\sqrt{1-\cos q}}{\sqrt{2+\cos\frac{K}{2}\,(1-\cos q)}} \\ &+\frac{1-\cos\frac{K}{2}}{\pi\sqrt{\cos\frac{K}{2}}}\ln\left(\pi\sqrt{2\cos\frac{K}{2}}\right)+\cos\frac{K}{2}+\frac{1-\cos\frac{K}{2}}{\pi\sqrt{\cos\frac{K}{2}}} \\ &\times\int_0^\pi dq\left\{\frac{1+\cos\frac{K}{2}\,(1-\cos q)}{\sqrt{(1-\cos q)\left[2+\cos\frac{K}{2}\,(1-\cos q)\right]}}-\frac{1}{q}\right\}. \end{aligned} \tag{5.3.19}$$

The calculation of B_{yy} is similar to that of B_{xy} and gives

$$B_{yy} = -\frac{1}{\pi}\int_0^\pi dq \frac{\cos q\sqrt{1-\cos q}}{\sqrt{2\cos\frac{K}{2}+1-\cos q}}. \tag{5.3.20}$$

Replacing Eqs. (5.3.15)–(5.3.20) into Eq. (5.3.6), we obtain the equation for the bound state near the bottom of the two-magnon band along the $(1,0)$-direction

$$\frac{1-\cos\frac{K}{2}}{4\pi S\sqrt{\cos\frac{K}{2}}}\ln\epsilon\left(1-\frac{B_{yy}-B_{xy}}{2S}\right)+\left(1-\frac{B_{xx}^{\rm reg}}{2S}\right)\left(1-\frac{B_{yy}}{2S}\right)-\frac{1}{4S^2}B_{xy}B_{yx}^{\rm reg}=0. \tag{5.3.21}$$

The solution of Eq. (5.3.21) is

$$\epsilon = \exp\left[-\frac{4\pi S\sqrt{\cos\frac{K}{2}}}{1-\cos\frac{K}{2}}\ f(K,S)\right] \tag{5.3.22}$$

where

$$f(K,S) = \frac{\left(1-\frac{B_{xx}^{\rm reg}}{2S}\right)\left(1-\frac{B_{yy}}{2S}\right)-\frac{B_{xy}B_{yx}^{\rm reg}}{4S^2}}{1-\frac{B_{yy}-B_{xy}}{2S}}. \tag{5.3.23}$$

In the limit of small wavevectors from Eqs. (5.3.16), (5.3.17), (5.3.19) and (5.3.20), one obtains

$$B_{xx}^{\rm reg} = B_{yy} = -\frac{1}{\pi}\int_0^\pi dq\cos q\left(\frac{1-\cos q}{3-\cos q}\right)^{1/2}+O(K^2) \tag{5.3.24}$$

and

$$B_{yx}^{\rm reg} = B_{xy} = 1-\frac{1}{\pi}\int_0^\pi dq\,(2-\cos q)\left(\frac{1-\cos q}{3-\cos q}\right)^{1/2}+O(K^2). \tag{5.3.25}$$

Then Eq. (5.3.23) becomes

$$f(K,S) = 1 - \frac{1}{2S}\left[1 - \frac{2}{\pi}\int_0^\pi dq \left(\frac{1-\cos q}{3-\cos q}\right)^{1/2}\right] + O(K^2) = 1 + O(K^2). \tag{5.3.26}$$

The integral in Eq. (5.3.26) is easily evaluated by using the change of variable $\cos\frac{q}{2} = \xi$ and its value is $\frac{\pi}{2}$. Then

$$\epsilon \simeq \exp\left[-\frac{32\pi S}{K^2}\right]. \tag{5.3.27}$$

The relationship (5.3.27) proves that for small wavevectors, the energy of the bound state is below the bottom of the two-magnon bound states by an exponentially small amount which explains why the bound state and the bottom of the two-magnon band are indistinguishable in the right panel of Fig. 5.2.

Let us conclude this section looking for the bound states with $\boldsymbol{K} = (K, K)$. From Eqs. (5.3.1)–(5.3.4) one obtains $B_{xx} = B_{yy}$, $B_{xy} = B_{yx}$ so that the bound state equation (5.3.6) splits into the couple of equations

$$1 - \frac{1}{2S}(B_{xx} + B_{xy}) = 0 \tag{5.3.28}$$

and

$$1 - \frac{1}{2S}(B_{xx} - B_{xy}) = 0 \tag{5.3.29}$$

where

$$B_{xx} + B_{xy} = 1 \pm \frac{x}{\pi\cos\frac{K}{2}}\int_0^\pi dq \frac{\cos\frac{K}{2} - \cos q}{\sqrt{\left(x + \cos\frac{K}{2}\cos q\right)^2 - \cos^2\frac{K}{2}}} \tag{5.3.30}$$

and

$$B_{xx} - B_{xy} = -1 \mp \frac{1}{\pi\cos\frac{K}{2}}\int_0^\pi dq \frac{\left(\cos\frac{K}{2} - \cos q\right)\left(x + 2\cos\frac{K}{2}\cos q\right)}{\sqrt{\left(x + \cos\frac{K}{2}\cos q\right)^2 - \cos^2\frac{K}{2}}}. \tag{5.3.31}$$

where the upper (lower) sign holds for $x < -2\cos\frac{K}{2}$ ($x > 2\cos\frac{K}{2}$). The solutions of Eqs. (5.3.28), (5.3.29) exist only for $x < -2\cos\frac{K}{2}$, that is for energies below the two-magnon band. In particular, for $x = -2\cos\frac{K}{2}$ (the value of the bound state energy when it meets the bottom of the two-magnon band), Eq. (5.3.30) becomes

$$B_{xx} + B_{xy} = 1 - \frac{2}{\pi\cos\frac{K}{2}}\int_0^\pi dq \frac{\cos\frac{K}{2} - \cos q}{\sqrt{(3-\cos q)(1-\cos q)}} \to +\infty \tag{5.3.32}$$

for any K so that one solution of Eq. (5.3.28) always exists implying that one bound state exists over the whole $(1,1)$-direction. Analagously, for $x = -2\cos\frac{K}{2}$, Eq. (5.3.31) gives

$$B_{xx} - B_{xy} = -1 - \frac{1}{\pi\cos\frac{K_c}{2}}\int_0^\pi dq \frac{\left(\cos\frac{K_c}{2} - \cos q\right)(1-\cos q)}{\sqrt{(3-\cos q)(1-\cos q)}} = \frac{1}{\cos\frac{K_c}{2}}\left(\frac{4}{\pi} - 1\right). \tag{5.3.33}$$

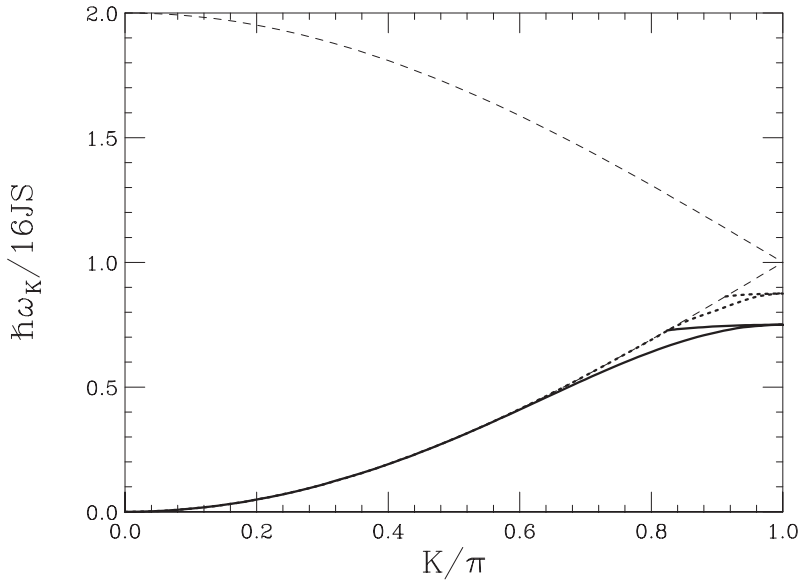

Fig. 5.3. Two-magnon bound state energy versus wavevector along the (1,1)-direction for a SQ lattice. The light dashed lines represent the top and the bottom of the two-magnon band. The continuous and dotted curves represent the two bound states for $S = 1/2$ and 1 respectively.

The integral in Eq. (5.3.33) has been evaluated analytically, performing the change of variable $\xi = \cos\frac{q}{2}$. The replacement of Eq. (5.3.33) into Eq. (5.3.29) shows that one solution exists only for $K > K_c(S)$ where

$$K_c(S) = 2\arccos\left[\frac{1}{2S}\left(\frac{4}{\pi} - 1\right)\right], \tag{5.3.34}$$

so that the existence of a second bound state is restricted to a region close to the ZC as shown in the left panel of Fig. 5.2 for $S = 1/2$. From Eq. (5.3.34), one has $K_c(S) = 0.82381\pi, 0.91275\pi, 0.94194\pi, 0.95648\pi, 0.96519\pi, 0.97100\pi, \ldots$, for $S = \frac{1}{2}, 1, \frac{3}{2}, 2, \frac{5}{2}, 3, \ldots$, respectively, showing that the region of existence of this second bound state decreases, increasing the spin value. In Fig. 5.3, the bound states in a SQ lattice versus the reduced wavevector $\frac{K}{\pi}$ along the $(1,1)$-direction are shown for $S = \frac{1}{2}$ (continuous curve) and 1 (dotted curve) respectively. Two bound states exist for $K > 0.82381\pi$ ($S = \frac{1}{2}$) and for $K > 0.91275\pi$ ($S = 1$). For $K = K_c(S)$, one bound state enters the continuum of the two-magnon band while the other bound state exists for any K and any S. Notice that for $K \lesssim 0.7\pi$ ($S = \frac{1}{2}$) and $K \lesssim 0.8\pi$ ($S = 1$), the bound state is so close to the bottom of the two-magnon band that it is indistinguishable from the bottom of the band. An analytic solution of equation (5.3.28) leads to[39]

$$x \simeq -2\cos\frac{K}{2}\left[1 + 8e^{-\pi}\exp\left(-\frac{2\pi S\cos\frac{K}{2}}{1-\cos\frac{K}{2}}\right)\right]. \tag{5.3.35}$$

Notice that there is a slight difference with Eq. (67) of Wortis[39] where a factor $e^{-\pi}$ is missing. The bound state energy is below the two-magnon band by an amount

$$\Delta(K) = \frac{\hbar\omega_{\rm bottom} - \hbar\omega_{\rm BS}}{16JS} \simeq 8e^{-\pi}\cos\frac{K}{2}\exp\left(-\frac{2\pi S\cos\frac{K}{2}}{1-\cos\frac{K}{2}}\right) \tag{5.3.36}$$

that is less than 2×10^{-4} for $K < \pi/2$ ($S = 1/2$) and less than 2×10^{-3} for $K < 0.8\pi$ ($S = 1$) explaining the failed resolution of the bound states from the bottom of the two-magnon band in Fig. 5.3.

Let us conclude this section by coming back to Fig. 5.2 where the bound states for a SQ lattice with $S = 1/2$ are shown in several directions of the reciprocal space. At least one bound state exists for any $\boldsymbol{K}$ below the two-magnon band. Along the $(1,1)$-direction, one further bound state appears close to the ZC ($0.82381 < K/\pi < 1$). Along the boundary of the Brillouin zone (π, K) and (K, π), two bound states exist for any wavevector while along the $(1,0)$ and $(0,1)$ directions, only one bound state is found. This scenario is qualitatively the same for other 2D lattice as, for instance, the triangular (TR) lattice.[40]

5.4. Bound States in 3D

In a SC lattice the bound states are obtained as solutions of Eq. (5.1.4) with $B_{\alpha\beta}$, $\alpha,\beta = x,y,z$ given by Eq. (5.1.5) and $x = \frac{\hbar\omega}{8JS} - 3$. There are no solution for energy above the top of the two-magnon band. For energies below the bottom of the two-magnon band $\hbar\omega_{\rm bottom} = 24JS[1 - \frac{1}{3}(\cos\frac{K_x}{2} + \cos\frac{K_y}{2} + \cos\frac{K_z}{2})]$, the sums defining $B_{\alpha\beta}$ may be reduced to 2D integrals that can be evaluated numerically. We will investigate in this section the existence of bound states in several directions of the first BZ of the reciprocal lattice.

For $\boldsymbol{K} = (K,K,K)$, the nine $B_{\alpha\beta}$ of Eq. (5.1.5) reduce to B_{xx} and B_{xy}: indeed, one has $B_{xx} = B_{yy} = B_{zz}$ and $B_{xy} = B_{yx} = B_{xz} = B_{zx} = B_{yz} = B_{zy}$ where

$$B_{xx} = -\frac{1}{\pi^2}\int_0^\pi dq_x \int_0^\pi dq_y \frac{\cos q_x\left(\cos\frac{K}{2} - \cos q_x\right)}{\sqrt{\left[x + \cos\frac{K}{2}\left(\cos q_x + \cos q_y\right)\right]^2 - \cos^2\frac{K}{2}}} \tag{5.4.1}$$

and

$$B_{xy} = -\frac{1}{\pi^2}\int_0^\pi dq_x \int_0^\pi dq_y \frac{\cos q_x\left(\cos\frac{K}{2} - \cos q_y\right)}{\sqrt{\left[x + \cos\frac{K}{2}\left(\cos q_x + \cos q_y\right)\right]^2 - \cos^2\frac{K}{2}}}. \tag{5.4.2}$$

The bound state equation (5.1.4) reduces to

$$\left[1 - \frac{1}{2S}\left(B_{xx} - B_{xy}\right)\right]^2\left[1 - \frac{1}{2S}\left(B_{xx} + 2B_{xy}\right)\right] = 0 \tag{5.4.3}$$

so that there are two degenerate bound states for

$$\left[1 - \frac{1}{2S}\left(B_{xx} - B_{xy}\right)\right] = 0 \tag{5.4.4}$$

and one bound state for

$$\left[1-\frac{1}{2S}\left(B_{xx}+2B_{xy}\right)\right]=0. \tag{5.4.5}$$

Note that for $K=\pi$, both Eqs. (5.4.4) and (5.4.5) reduce to

$$\left(1+\frac{1}{4xS}\right)=0 \tag{5.4.6}$$

so that at the ZC three degenerate bound states exist with energy

$$\hbar\omega_{\rm BS}(\pi,\pi,\pi)=24JS\left(1-\frac{1}{12S}\right). \tag{5.4.7}$$

For $K<\pi$, one sees that Eqs. (5.4.4) and (5.4.5) do not always have solution. In particular, the doubly degenerate bound state, solution of Eq. (5.4.4) exists only for $K_c^{(2)}<K<\pi$ and the existence of the single bound state coming from the solution of Eq. (5.4.5) is limited to the region $K_c^{(1)}<K<\pi$, where $K_c^{(2)}$ and $K_c^{(1)}$ can be determined by evaluating the combinations $B_{xx}-B_{yy}$ and $B_{xx}+2B_{xy}$ for $x=-3\cos\frac{K}{2}$, corresponding to the value of x when the bound state meets the bottom of the two-magnon band. One obtains

$$B_{xx}-B_{xy}=\frac{1}{\pi^2\cos\frac{K}{2}}\int_0^\pi dq_x\int_0^\pi dq_y\frac{\cos q_x\left(\cos q_x-\cos q_y\right)}{\sqrt{\left(3-\cos q_x-\cos q_y\right)^2-1}}=\frac{0.185237}{\cos\frac{K}{2}} \tag{5.4.8}$$

and using Eq. (5.4.4) one finds

$$K_c^{(2)}=2\arccos\left(\frac{0.185237}{2S}\right) \tag{5.4.9}$$

so that $K_c^{(2)}=0.88139\pi$ for $S=1/2$. Then

$$\begin{aligned}B_{xx}+2B_{xy}&=3\left(1-\cos\frac{K}{2}\right)\frac{1}{\pi^2\cos\frac{K}{2}}\int_0^\pi dq_x\int_0^\pi dq_y\frac{\cos q_x}{\sqrt{\left(3-\cos q_x-\cos q_y\right)^2-1}}\\&=0.516386\frac{1-\cos\frac{K}{2}}{\cos\frac{K}{2}}.\end{aligned} \tag{5.4.10}$$

Using Eq. (5.4.5), one obtains

$$K_c^{(1)}=2\arccos\left(\frac{0.516386}{2S+0.516386}\right) \tag{5.4.11}$$

so that $K_c^{(1)}=0.77878\pi$ for $S=1/2$. The bound states along the $(1,1,1)$-direction are shown in the first panel of Fig. 5.4 along with the bottom and the top of the two-magnon band (dashed curves). The existence of one bound state, solution of Eq. (5.4.5) (lower continuous curve), is restricted to the region $0.77878<K/\pi<1$ while the doubly degenerate bound state, solution of Eq. (5.4.4) (higher curve), exists only for $0.88139<K/\pi<1$. By increasing the spin S, the region of existence of both bound states is further reduced.

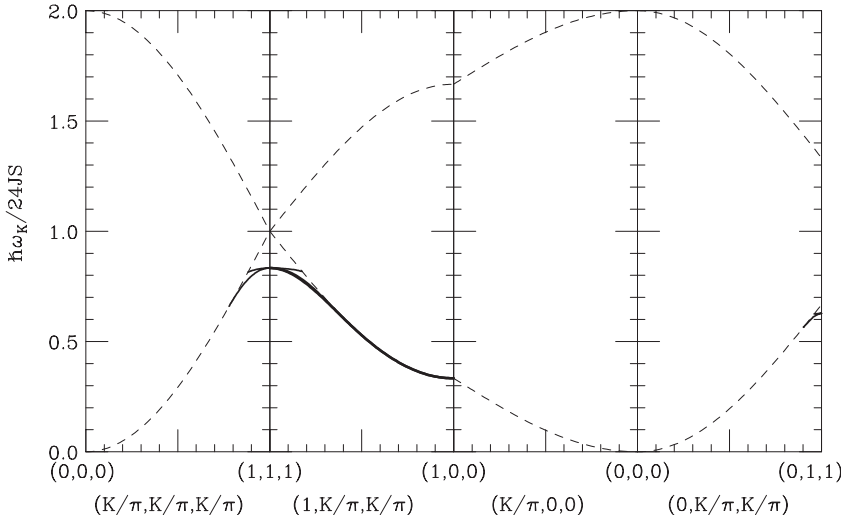

Fig. 5.4. Two-magnon bound state energy versus wavevector along four directions of a SC lattice with $S = 1/2$: (K, K, K) (first panel), (π, K, K) (second panel), $(K, 0, 0)$ (third panel) and $(0, K, K)$ (last panel). The dashed lines represent the top and the bottom of the two-magnon band. The continuous curves represent the bound states. The lower heavy curve in the second panel represents a couple of (non-degenerate) bound states with very close energies.

Now, we look for the bound states along the diagonals of the faces of the cube of the BZ. In particular, for $\boldsymbol{K} = (\pi, K, K)$, one has

$$B_{xx} = \frac{1}{2\pi}\int_0^\pi dq \frac{1}{\sqrt{\left(x + \cos\frac{K}{2}\cos q\right)^2 - \cos^2\frac{K}{2}}}, \tag{5.4.12}$$

$$B_{yy} = B_{zz} = -\frac{1}{\pi}\int_0^\pi dq \frac{\cos q\left(\cos\frac{K}{2} - \cos q\right)}{\sqrt{\left(x + \cos\frac{K}{2}\cos q\right)^2 - \cos^2\frac{K}{2}}}, \tag{5.4.13}$$

$B_{xy} = B_{yx} = B_{xz} = B_{zx} = 0$ and

$$B_{yz} = B_{zy} = 1 + \frac{1}{\pi\cos\frac{K}{2}}\int_0^\pi dq \frac{(\cos\frac{K}{2} - \cos q)(x + \cos\frac{K}{2}\cos q)}{\sqrt{(x + \cos\frac{K}{2}\cos q)^2 - \cos^2\frac{K}{2}}}. \tag{5.4.14}$$

The bound state equation (5.1.4) reduces to

$$\left(1 - \frac{1}{2S}B_{xx}\right)\left[1 - \frac{1}{2S}\left(B_{yy} - B_{yz}\right)\right]\left[1 - \frac{1}{2S}\left(B_{yy} + B_{yz}\right)\right] = 0 \tag{5.4.15}$$

so that the bound states are the possible solutions of the three equations

$$\left(1 - \frac{1}{2S}B_{xx}\right) = 0, \tag{5.4.16}$$

$$\left[1-\frac{1}{2S}\left(B_{yy}-B_{yz}\right)\right]=0 \tag{5.4.17}$$

and

$$\left[1-\frac{1}{2S}\left(B_{yy}+B_{yz}\right)\right]=0. \tag{5.4.18}$$

Equations (5.4.16) and (5.4.18) have one solution for any K since B_{xx} and $B_{yy}+B_{yz}$ diverge for $x\to -2\cos\frac{K}{2}$, whereas Eq. (5.4.17) has one solution only for $K_c<K<\pi$. To find K_c, since $B_{yy}-B_{yz}$ is finite at $x=-2\cos\frac{K}{2}$

$$B_{yy}-B_{yz}=\frac{1}{\cos\frac{K}{2}}\left(\frac{4}{\pi}-1\right). \tag{5.4.19}$$

Using Eq. (5.4.17), one has

$$K_c(S)=2\arccos\left[\frac{1}{2S}\left(\frac{4}{\pi}-1\right)\right] \tag{5.4.20}$$

and $K_c(\frac{1}{2})=0.82381\pi$. In the second panel of Fig. 5.4, the bound states obtained from Eqs. (5.4.16)–(5.4.18) are shown. The solution of Eq. (5.4.17) corresponds to the higher curve. The solutions of Eqs. (5.4.16) and (5.4.18) correspond to the apparently unique lower curve. The bound states, solutions of Eqs. (5.4.16) and (5.4.18), are degenerate only at $K=0$ and $K=\pi$. However, the energy difference between them for $0<K<\pi$ reaches its maximum $\hbar\omega=24JS\times 0.0055$ around $K\simeq 0.8\pi$. The proximity of these two bound states prevents any resolution between them using the scale of Fig. 5.4. Obviously, the same result is obtained for $\boldsymbol{K}=(K,\pi,K)$ and (K,K,π).

Now we look for the bound states along the edges of the cube. Assuming $\boldsymbol{K}=(K,0,0)$, we have

$$B_{xx}=-\frac{1}{\pi^2}\int_0^\pi dq_x\int_0^\pi dq_y\frac{\cos q_x\left(\cos\frac{K}{2}-\cos q_x\right)}{\sqrt{\left(x+\cos\frac{K}{2}\cos q_x+\cos q_y\right)^2-1}}, \tag{5.4.21}$$

$$B_{yy}=B_{zz}=-\frac{1}{\pi^2}\int_0^\pi dq_y\int_0^\pi dq_z\frac{\cos q_y\left(1-\cos q_y\right)}{\sqrt{\left(x+\cos q_y+\cos q_z\right)^2-\cos^2\frac{K}{2}}}, \tag{5.4.22}$$

$$B_{xy}=B_{xz}=-\frac{1}{\pi^2}\int_0^\pi dq_x\int_0^\pi dq_y\frac{\cos q_x\left(1-\cos q_y\right)}{\sqrt{\left(x+\cos\frac{K}{2}\cos q_x+\cos q_y\right)^2-1}}, \tag{5.4.23}$$

$$B_{yx}=B_{zx}=-\frac{1}{\pi^2}\int_0^\pi dq_x\int_0^\pi dq_y\frac{\cos q_y\left(\cos\frac{K}{2}-\cos q_x\right)}{\sqrt{\left(x+\cos\frac{K}{2}\cos q_x+\cos q_y\right)^2-1}}, \tag{5.4.24}$$

$$B_{yz} = B_{zy} = -\frac{1}{\pi^2}\int_0^\pi dq_y \int_0^\pi dq_z \frac{\cos q_y\,(1-\cos q_z)}{\sqrt{\left(x+\cos q_y+\cos q_z\right)^2-\cos^2\frac{K}{2}}}. \tag{5.4.25}$$

The bound state equation (5.1.4) reduces to

$$\left[1-\frac{1}{2S}\left(B_{yy}-B_{yz}\right)\right]\left\{\left(1-\frac{1}{2S}B_{xx}\right)\left[1-\frac{1}{2S}\left(B_{yy}+B_{yz}\right)\right]-\frac{1}{2S^2}B_{xy}B_{yx}\right\}=0. \tag{5.4.26}$$

A numerical evaluation of the integrals (5.5.21)–(5.5.25) leads to the conclusion that both equations

$$1-\frac{1}{2S}\left(B_{yy}-B_{yz}\right)=0 \tag{5.4.27}$$

and

$$\left(1-\frac{1}{2S}B_{xx}\right)\left[1-\frac{1}{2S}\left(B_{yy}+B_{yz}\right)\right]-\frac{1}{2S^2}B_{xy}B_{yx}=0 \tag{5.4.28}$$

have no solution for any K, so that no bound state exists along the $(1,0,0)$-direction as illustrated by the third panel of Fig. 5.4. The same result is obtained for $\boldsymbol{K} = (0,K,0)$ and $(0,0,K)$.

We conclude this section by evaluating the bound states for $\boldsymbol{K} = (0,K,K)$ for which $B_{yy} = B_{zz}$, $B_{xy} = B_{xz}$, $B_{yx} = B_{zx}$ and $B_{yz} = B_{zy}$. The bound state equation (5.1.4) becomes identical to Eq. (5.4.26) but with different $B_{\alpha\beta}$. In particular, we have

$$B_{xx} = -\frac{1}{\pi^2}\int_0^\pi dq_x \int_0^\pi dq_y \frac{\cos q_x\,(1-\cos q_x)}{\sqrt{\left(x+\cos q_x+\cos\frac{K}{2}\cos q_y\right)^2-\cos^2\frac{K}{2}}}, \tag{5.4.29}$$

$$B_{xy} = -\frac{1}{\pi^2}\int_0^\pi dq_x \int_0^\pi dq_y \frac{\cos q_x\left(\cos\frac{K}{2}-\cos q_y\right)}{\sqrt{\left(x+\cos q_x+\cos\frac{K}{2}\cos q_y\right)^2-\cos^2\frac{K}{2}}}, \tag{5.4.30}$$

$$B_{yx} = -\frac{1}{\pi^2}\int_0^\pi dq_x \int_0^\pi dq_y \frac{\cos q_y\,(1-\cos q_x)}{\sqrt{\left(x+\cos q_x+\cos\frac{K}{2}\cos q_y\right)^2-\cos^2\frac{K}{2}}}, \tag{5.4.31}$$

$$B_{yy} - B_{yz} = -\frac{1}{\pi^2}\int_0^\pi dq_y \int_0^\pi dq_z \frac{\cos q_y\,(\cos q_z-\cos q_y)}{\sqrt{\left[x+\cos\frac{K}{2}\left(\cos q_y+\cos q_z\right)\right]^2-1}}, \tag{5.4.32}$$

$$B_{yy} + B_{yz} = -\frac{1}{\pi^2}\int_0^\pi dq_y \int_0^\pi dq_z \frac{\cos q_y\left(2\cos\frac{K}{2}-\cos q_y-\cos q_z\right)}{\sqrt{\left[x+\cos\frac{K}{2}\left(\cos q_y+\cos q_z\right)\right]^2-1}} \tag{5.4.33}$$

with $-3 < x < -1 - 2\cos\frac{K}{2}$. For $K = \pi$, one obtains $B_{xy} = B_{yx} = 0$,

$$B_{xx} = (1+x)\left(1 + \frac{x}{\sqrt{x^2-1}}\right), \quad B_{yy} - B_{yz} = B_{yy} + B_{yz} = \frac{1}{2\sqrt{x^2-1}} \tag{5.4.34}$$

and Eq. (5.4.26) becomes

$$\left(1 - \frac{1}{4S\sqrt{x^2-1}}\right)^2 \left[1 - \frac{1}{2S}(1+x)\left(1 + \frac{x}{\sqrt{x^2-1}}\right)\right] = 0. \tag{5.4.35}$$

The first factor of Eq. (5.4.35) vanishes for

$$x = -\sqrt{1 + \frac{1}{16S^2}} \tag{5.4.36}$$

while the second factor does not vanish for any $-3 < x < -1$. The energy of the doubly degenerate bound state is

$$\hbar\omega_{\rm BS}(0,\pi,\pi) = 24JS\left(1 - \frac{1}{3}\sqrt{1 + \frac{1}{16S^2}}\right). \tag{5.4.37}$$

Moving away from $(0,\pi,\pi)$, the degenerate bound state splits into two distinct bound states: the first is the solution of Eq. (5.4.27) and exists for $K_c^{(1)} < K < \pi$ with $K_c^{(1)} = 0.96011\pi$ for $S = 1/2$; the second bound state is the solution of Eq. (5.4.28) and exists for $K_c^{(2)} < K < \pi$ with $K_c^{(2)} = 0.90227\pi$ for $S = 1/2$. The bound states for $\boldsymbol{K} = (0, K, K)$ are shown as continuous curves in the last panel of Fig. 5.4 along with the top and bottom of the two-magnon band (dashed curves). Obviously, the same result is obtained from the equivalent directions $\boldsymbol{K} = (K, 0, K)$ and $(K, K, 0)$.

In summary, the four panels of Fig. 5.4 show that the bound states of a SC isotropic ferromagnet are comprised between 0 and 3 depending on the wavevector $\boldsymbol{K}$. The novelty with respect to the results obtained for the 1D and 2D case is that in 3D, a wide region around $\boldsymbol{K} = (0,0,0)$ exists free of bound states. On the other hand, in a small region around $\boldsymbol{K} = (\pi,\pi,\pi)$, three bound states exist. Regions with one or two bound states are thin shells in the vicinity of the faces of the cube of the BZ. It should be noted that the qualitative shape of the regions with 0, 1, 2, 3 bound states was sketched by Wortis[39] in his fundamental paper *Bound states of two spin waves in the Heisenberg ferromagnet*. Figure 7 of that paper (reproduced by many textbooks on magnetism) is not quantitatively correct. Indeed, the region with zero bound states should be extended to the corners of the cube at the expense of the one bound state region which should be reduced to a thin space between the regions with zero and two bound states, respectively. This misrepresentation was induced by Fig. 6 of the same paper where the two bound states existing for any K along the (K, K, π) direction are clearly split off from each other and one of them (the lower in energy) does not merge into the continuum for $K \to 0$ in disagreement with the second panel of Fig. 5.4.

Concluding this section, we summarize the scenario of the two-magnon bound states in an isotropic Heisenberg ferromagnet: in all dimensions, the bound states exist only below the two-magnon band:

i) in 1D (linear chain) only one bound state exists for any wavevector $0 < K < \pi$;
ii) in 2D (square lattice[39] and triangular lattice[40]), one bound state exists for any wavevector, a second bound state exists only in a shell of the BZ near the boundaries;
iii) in 3D (simple cubic,[39] body centred cubic and face centred cubic[41] lattices), no bound state exists in a wide region around the zone centre while three bound states exist in a small region close to the zone corner $\boldsymbol{K} = (\pi, \pi, \pi)$.

5.5. Bound States in Anisotropic Ferromagnets

We have obtained in Sec. 1.7 the determinant equation (1.7.17) for a "cubic" anisotropic ferromagnet in the presence of single-ion easy-axis anisotropy ($D > 0$) and exchange easy-axis anisotropy ($J^z \geq J^\perp$)

$$\det \begin{pmatrix} 1 + \dfrac{D}{4J^\perp S} I_0 & \dfrac{J^z}{2J^\perp S} I_x & \dfrac{J^z}{2J^\perp S} I_y & \dfrac{J^z}{2J^\perp S} I_z \\ \dfrac{D}{4J^\perp S} A_x & 1 - \dfrac{1}{2S} B_{xx} & -\dfrac{1}{2S} B_{xy} & -\dfrac{1}{2S} B_{xz} \\ \dfrac{D}{4J^\perp S} A_y & -\dfrac{1}{2S} B_{yx} & 1 - \dfrac{1}{2S} B_{yy} & -\dfrac{1}{2S} B_{yz} \\ \dfrac{D}{4J^\perp S} A_z & -\dfrac{1}{2S} B_{zx} & -\dfrac{1}{2S} B_{zy} & 1 - \dfrac{1}{2S} B_{zz} \end{pmatrix} = 0, \qquad (5.5.1)$$

where I_0, I_α, A_α and $B_{\alpha\beta}$ are given by Eqs. (1.7.13)–(1.7.15) and (1.7.18)–(1.7.19). As one can see from Eq. (5.5.1), the exchange anisotropy alone does not change the number of roots of the determinant equation: indeed for $D = 0$, Eq. (5.5.1) reduces to

$$\det \left[\mathbf{1} - \frac{1}{2S} \mathbf{B}(\boldsymbol{K}, \omega) \right] = 0 \qquad (5.5.2)$$

that looks similar to the determinant equation obtained for the isotropic case given in Eq. (5.1.4). However, the matrix elements differ from the isotropic case because of the factor $J^z/J^\perp$ in $B_{\alpha\beta}$ given by Eq. (1.7.19). In any case, the number of bound states is the same as in the isotropic case even though their energy is changed. On the contrary, the single-ion anisotropy increases the dimension of the determinant entering a new bound state. At the ZC ($K_\alpha = \pi$), one has $I_0 = \frac{1}{x}$, $I_\alpha = 0$, $A_\alpha = 0$ and $B_{\alpha\beta} = -\frac{J^z}{2J^\perp x} \delta_{\alpha,\beta}$ so that Eq. (5.5.1) reduces to

$$\left(1 + \frac{D}{4J^\perp S x} \right) \left(1 + \frac{J^z}{4J^\perp S x} \right)^3 = 0 \qquad (5.5.3)$$

and from Eq. (1.7.11), the bound state energies become

$$\hbar\omega_{\rm BS}^{\rm (s)}(\pi,\pi,\pi) = 2h + 2D(2S-1) + 8J^{\perp}S - 2D \tag{5.5.4}$$

with $G^{0}_{\pi,\pi,\pi} = 1$, $G^{\alpha}_{\pi,\pi,\pi} = 0$ ($\alpha = x, y, z$) and

$$\hbar\omega_{\rm BS}^{\rm (ex)}(\pi,\pi,\pi) = 2h + 2D(2S-1) + 8J^{\perp}S - 2J^{z} \tag{5.5.5}$$

with $G^{0}_{\pi,\pi,\pi} = 0$, $G^{\alpha}_{\pi,\pi,\pi} = 1$ ($\alpha = x, y$ or z). The superscripts "s" and "ex" stay for "single-ion" and "exchange" bound states.[42] Using Eqs. (1.7.10) and (1.4.11), one has

$$F_{\boldsymbol{K}}(\boldsymbol{r}) = -\frac{1}{N}\sum_{\boldsymbol{q}}\left(\frac{D}{4J^{\perp}S}G^{0}_{\boldsymbol{K}} + \frac{J^{z}}{2J^{\perp}S}\sum_{\alpha}G^{\alpha}_{\boldsymbol{K}}\cos q_{\alpha}\right)\frac{\cos\boldsymbol{q}\cdot\boldsymbol{r}}{x + \sum_{\sigma}\cos\frac{K_{\sigma}}{2}\cos q_{\sigma}} \tag{5.5.6}$$

so that

$$F^{\rm (s)}_{\pi,\pi,\pi}(\boldsymbol{r}) = \frac{1}{N}\sum_{\boldsymbol{q}}\cos\boldsymbol{q}\cdot\boldsymbol{r} = \delta_{\boldsymbol{r},0} \tag{5.5.7}$$

for the single-ion bound state (5.5.4) and

$$F^{\rm (ex)}_{\pi,\pi,\pi}(\boldsymbol{r}) = \frac{2}{N}\sum_{\boldsymbol{q}}\cos\boldsymbol{q}\cdot\boldsymbol{\delta}\cos\boldsymbol{q}\cdot\boldsymbol{r} = \delta_{\boldsymbol{r},\boldsymbol{\delta}} \tag{5.5.8}$$

for the triply degenerate exchange bound state (5.5.5). In Eq. (5.5.8), $\boldsymbol{\delta}$ is a vector connecting two NN spins. The probability of finding the two spin deviations on the same lattice site is obtained from Eq. (1.4.34) that reads

$$P^{\rm (s)}_{\pi,\pi,\pi}(0) = 1 \tag{5.5.9}$$

for the single-ion bound state and

$$P^{\rm (ex)}_{\pi,\pi,\pi}(0) = 0 \tag{5.5.10}$$

for the exchange bound state. On the other hand, the probability of finding the two spin deviations on lattice sites connected by a vector $\boldsymbol{r}$ is obtained from Eq. (1.4.35) that reads

$$P^{\rm (s)}_{\pi,\pi,\pi}(\boldsymbol{r}) = 0 \tag{5.5.11}$$

for the single-ion bound state and

$$P^{\rm (ex)}_{\pi,\pi,\pi}(\boldsymbol{r}) = \delta_{\boldsymbol{r},\boldsymbol{\delta}} \tag{5.5.12}$$

for the exchange bound state. From Eqs. (5.5.9) and (5.5.11), one sees that the single-ion bound state corresponds to a state with two spin deviations on the same site. Analogously from Eqs. (5.5.10) and (5.5.12), one sees that the exchange bound state corresponds to a state with two spin deviations on NN sites. This classification is fully justified at the ZC but it becomes less meaningful as one moves away from

the ZC. To see this, we will perform explicit calculations for the 1D case for which Eqs. (5.5.1) and (5.5.6) reduce to

$$
\begin{aligned}
&f(x,K)\\
&\equiv \det\begin{pmatrix} 1+\dfrac{D}{4J^{\perp}S}I_0 & \dfrac{J^z}{2J^{\perp}S}\dfrac{1-xI_0}{\cos\frac{K}{2}} \\ \dfrac{D}{4J^{\perp}S}\dfrac{1-xI_0-\frac{J^z}{J^{\perp}}I_0\cos^2\frac{K}{2}}{\cos\frac{K}{2}} & 1-\dfrac{1}{2S}\left(1+\dfrac{J^z}{J^{\perp}}\dfrac{x}{\cos^2\frac{K}{2}}\right)(1-xI_0)\end{pmatrix}\\
&=0
\end{aligned}
\tag{5.5.13}
$$

and

$$
F_K(r)=-\frac{1}{\pi}\int_0^{\pi}dq\frac{\cos(r\ q)}{x_{\rm BS}+\cos\frac{K}{2}\cos q}\left(\frac{D}{4J^{\perp}S}G_K^0+\frac{J^z}{2J^{\perp}S}G_K^1\ \cos q\right), \tag{5.5.14}
$$

respectively. In Eq. (5.5.14), we have written explicitly $x_{\rm BS}$ instead of x to stress that it is a root of the determinant equation (5.5.13). For $x<-\cos\frac{K}{2}$ (bound states below the two magnon band) one has

$$
I_0=-\frac{1}{\sqrt{x^2-\cos^2\frac{K}{2}}} \tag{5.5.15}
$$

and Eq. (5.5.13) has two roots for $K_c<K\leq\pi$ and one root for $0<K\leq K_c$ where

$$
K_c=2\arccos\left[\frac{D+2J^z}{4J^{\perp}}-\sqrt{\left(\frac{D+2J^z}{4J^{\perp}}\right)^2-\frac{D\ J^z}{4(J^{\perp})^2S}}\right]. \tag{5.5.16}
$$

Equation (5.5.16) is obtained by evaluating Eq. (5.5.13) for $x=-\cos\frac{K}{2}-\epsilon$ and taking the limit $\epsilon\to 0$. For $\epsilon\to 0$, Eq. (5.5.13) becomes

$$
\frac{A}{\sqrt{2\epsilon}}+B+O(\sqrt{\epsilon})=0 \tag{5.5.17}
$$

where

$$
A=\frac{\cos^2\frac{K}{2}-\frac{D+2J^z}{2J^{\perp}}\cos\frac{K}{2}+\frac{D\ J^z}{4(J^{\perp})^2S}}{2S\cos^{3/2}\frac{K}{2}} \tag{5.5.18}
$$

and

$$
B=\frac{(2S-1)\cos^2\frac{K}{2}+\frac{J^z}{J^{\perp}}\cos\frac{K}{2}-\frac{D\ J^z}{4(J^{\perp})^2S}}{2S\cos^2\frac{K}{2}}. \tag{5.5.19}
$$

For $\epsilon\to 0$, the left-hand side of Eq. (5.5.17) diverges to $+\infty$ for $A>0$ ($K>K_c$) and to $-\infty$ for $A<0$ ($K<K_c$) where K_c is the root of the equation $A=0$. For $K=K_c$ ($A=0$), Eq. (5.5.19) goes to a finite value $B(K_c)<0$. These results imply that the function $f(x,K)$ of Eq. (5.5.13) crosses twice the x-axis for $K>K_c$ starting from 1 when $x\to-\infty$, becoming negative in a region $x_1<x<x_2$ and diverging to $+\infty$ for $x\to-\cos\frac{K}{2}$. On the contrary, for $K<K_c$ the function $f(x,K)$ crosses the

x-axis in one point x_1 going from 1 when $x \to -\infty$ to $-\infty$ in the limit $x \to -\cos\frac{K}{2}$. For $K = K_c$, the function $f(x, K_c)$ does not diverge for $x \to -\cos\frac{K_c}{2}$: it goes to the finite value $B(K_c) < 0$ and crosses the x-axis only once at the point x_1.

For $x > \cos\frac{K}{2}$ (possible bound states above the two-magnon band), one has

$$I_0 = \frac{1}{\sqrt{x^2 - \cos^2\frac{K}{2}}} \tag{5.5.20}$$

and the function $f(x, K)$ never crosses the x-axis being a monotonic function of x going from $+\infty$ for $x \to \cos\frac{K}{2}$ to 1 for $x \to \infty$. This means that Eq. (5.5.13) has no solution for $x > \cos\frac{K}{2}$, preventing the presence of bound states above the continuum. From Eqs. (5.2.12) and (5.5.14), one obtains

$$F_K(r) = -\frac{1}{\cos\frac{K}{2}} \left\{ \frac{J^z}{2J^\perp S}\delta_{r,0} G_K^1 + \left(\frac{D\cos\frac{K}{2}}{4J^\perp S x} G_K^0 - \frac{J^z}{2J^\perp S} G_K^1 \right) \right.$$
$$\left. \times \frac{1}{\sqrt{1 - \frac{\cos^2\frac{K}{2}}{x_{\rm BS}^2}}} \left[-\frac{x_{\rm BS}}{\cos\frac{K}{2}} \left(1 - \sqrt{1 - \frac{\cos^2\frac{K}{2}}{x_{\rm BS}^2}} \right) \right]^{|r|} \right\}. \tag{5.5.21}$$

The constants G_K^0 and G_K^1 are the two components of the eigenvector belonging to the eigenvalue $x_{\rm BS}$ according to the determinant equation (5.5.13). Writing G_K^0 and G_K^1 in terms of the arbitrary constant $F_K(1)$, Eq. (5.5.21) becomes

$$F_K(0) \left(x_{\rm BS} + \frac{D}{4J^\perp S} \right) = -F_K(1) \cos\frac{K}{2} \tag{5.5.22}$$

for $r = 0$ and

$$F_K(r) = F_K(1) \left(-\frac{x_{\rm BS} + \sqrt{x_{\rm BS}^2 - \cos^2\frac{K}{2}}}{\cos\frac{K}{2}} \right)^{|r|-1} \tag{5.5.23}$$

for $|r| \geq 2$. The probability of finding two spin deviations on the same site (1.4.34) or on different sites (1.4.35) becomes

$$P_K(0) = \frac{\left(1 - \frac{1}{2S}\right)\cos^2\frac{K}{2} \left[1 - \frac{x_{\rm BS}^2}{\cos^2\frac{K}{2}} \left(1 - \sqrt{1 - \frac{\cos^2\frac{K}{2}}{x_{\rm BS}^2}} \right)^2 \right]}{\left(1 - \frac{1}{2S}\right)\cos^2\frac{K}{2} \left[1 - \frac{x_{\rm BS}^2}{\cos\frac{K}{2}} \left(1 - \sqrt{1 - \frac{\cos^2\frac{K}{2}}{x_{\rm BS}^2}} \right)^2 \right] + \left(x_{\rm BS} + \frac{D}{4J^\perp S} \right)^2} \tag{5.5.24}$$

and

$$P_K(r) = \frac{\left(x_{\rm BS}+\frac{D}{4J^\perp S}\right)^2\left[1-\frac{x_{\rm BS}^2}{\cos^2\frac{K}{2}}\left(1-\sqrt{1-\frac{\cos^2\frac{K}{2}}{x_{\rm BS}^2}}\right)^2\right]\left[\frac{x_{\rm BS}}{\cos\frac{K}{2}}\left(1-\sqrt{1-\frac{\cos^2\frac{K}{2}}{x_{\rm BS}^2}}\right)\right]^{2(r-1)}}{\left(1-\frac{1}{2S}\right)\cos^2\frac{K}{2}\left[1-\frac{x_{\rm BS}^2}{\cos\frac{K}{2}}\left(1-\sqrt{1-\frac{\cos^2\frac{K}{2}}{x_{\rm BS}^2}}\right)^2\right]+\left(x_{\rm BS}+\frac{D}{4J^\perp S}\right)^2} \tag{5.5.25}$$

for $r \geq 1$. Notice that for $S = 1/2$, the probability (5.5.24) vanishes and the probability (5.5.25) becomes independent of D. This result should have been expected since the double occupancy is forbidden for $S = 1/2$ and the single-ion contribution to the anisotropy Hamiltonian reduces to a constant $-D\sum_i (S_i^z)^2 = -\frac{1}{4}DN$ so that D cannot occur in the spin dynamics.

For $K \to \pi$, we may expand Eq. (5.5.13) in powers of $\cos\frac{K}{2}$ and the solutions are given by

$$x_{\rm BS}^{(1)} = -\frac{J^z}{4J^\perp S}\left\{1+\frac{4(J^\perp)^2S\left[(3S-1)J^z-DS\right]}{(J^z)^2(J^z-D)}\cos^2\frac{K}{2} + \frac{16(J^\perp)^4S^2(2S-1)\left[3DJ^zS-D^2S-(4S-1)(J^z)^2\right]}{(J^z)^3(J^z-D)^3}\cos^4\frac{K}{2} + O\left(\cos^6\frac{K}{2}\right)\right\} \tag{5.5.26}$$

and

$$x_{\rm BS}^{(2)} = -\frac{D}{4J^\perp S}\left\{1-\frac{4(J^\perp)^2S(2S-1)}{D(J^z-D)}\cos^2\frac{K}{2} + \frac{16(J^\perp)^4S^2(2S-1)\left[D(S-1)+J^zS\right]}{D^2(J^z-D)^3}\cos^4\frac{K}{2}+O\left(\cos^6\frac{K}{2}\right)\right\}. \tag{5.5.27}$$

The probability of finding two spin deviations on the same site is given by

$$P_{K\to\pi}^{(1)}(0) = \frac{8(J^\perp)^2S(2S-1)}{(J^z-D)^2}\cos^2\frac{K}{2} - \frac{32(J^\perp)^4S^2(2S-1)[D^2S-4DJ^zS+(11S-4)(J^z)^2]}{(J^z)^2(J^z-D)^4}\cos^4\frac{K}{2} + O\left(\cos^6\frac{K}{2}\right) \tag{5.5.28}$$

for the bound state given by Eq. (5.5.26) and

$$P^{(2)}_{K\to\pi}(0) = 1 - \frac{2(J^\perp)^2 S(2S-1)}{(J^z-D)^2}\cos^2\frac{K}{2} + \frac{4(J^\perp)^4 S^2(2S-1)[D^2(4S-5)+8DJ^zS-2(J^z)^2S]}{D^2(J^z-D)^4}\cos^4\frac{K}{2} + O\left(\cos^6\frac{K}{2}\right) \tag{5.5.29}$$

for the bound state given by Eq. (5.5.27). Obviously, the probability of finding the two spin deviations on distinct lattice sites is $\sum_{r\neq 0} P_K(r) = 1 - P_K(0)$. As one can see from Eqs. (5.5.28) and (5.5.29), the bound state $x^{(1)}_{\rm BS}$ is an exchange bound state since $P^{(1)}_K(0) \to 0$ for $K \to \pi$ while the bound state $x^{(2)}_{\rm BS}$, is a single-ion bound state since $P^{(2)}_K(0) \to 1$ for $K \to \pi$. As previously announced, the exchange or single-ion nature of the bound state is rigorously confirmed only for $K = \pi$. Moving away from the zone boundary, a mixing between the exchange and single-ion characters occurs.

In the absence of single-ion anisotropy ($D = 0$), a single bound state exists. In particular, for $S = 1/2$, the energy of the two-magnon bound state is given by

$$\hbar\omega_{\rm BS} = 2h + 2J^z\left[1 - \left(\frac{J^\perp}{J^z}\right)^2\cos^2\frac{K}{2}\right] \tag{5.5.30}$$

that in the Heisenberg limit ($J^z = J^\perp$) reduces to the isotropic result given in Eq. (5.2.6) and in the Ising limit ($J^\perp = 0$) reduces to

$$\hbar\omega_{\rm BS} = 2h + 2J^z. \tag{5.5.31}$$

The result (5.5.31) represents the energy cost of a couple of NN spin reversals. The bound state (5.5.30) is always below the bottom of the two-magnon band

$$\hbar\omega_{\rm bottom} = 2h + 4J^z\left(1 - \frac{J^\perp}{J^z}\cos\frac{K}{2}\right) \tag{5.5.32}$$

and crosses the single-spin wave spectrum

$$\hbar\omega = h + 2J^z\left(1 - \frac{J^\perp}{J^z}\cos k\right) \tag{5.5.33}$$

at

$$K_{\rm cross} = \arccos\frac{J^\perp - h\frac{J^z}{J^\perp}}{2J^z - J^\perp}. \tag{5.5.34}$$

For $K < K_{\rm cross}$, the single-spin wave excitation is the lowest excited state while for $K > K_{\rm cross}$, the bound state is the lowest excitation. In the Heisenberg limit, $J^\perp = J^z$, one has $K_{\rm cross} = \arccos(1 - h/J^z)$ and the bound state becomes the lowest excitation for any $0 < K < \pi$ only when $h = 0$. The result for $S \neq 1/2$ is

qualitatively similar to the result obtained for $S = 1/2$ even though only numerical results can be obtained.

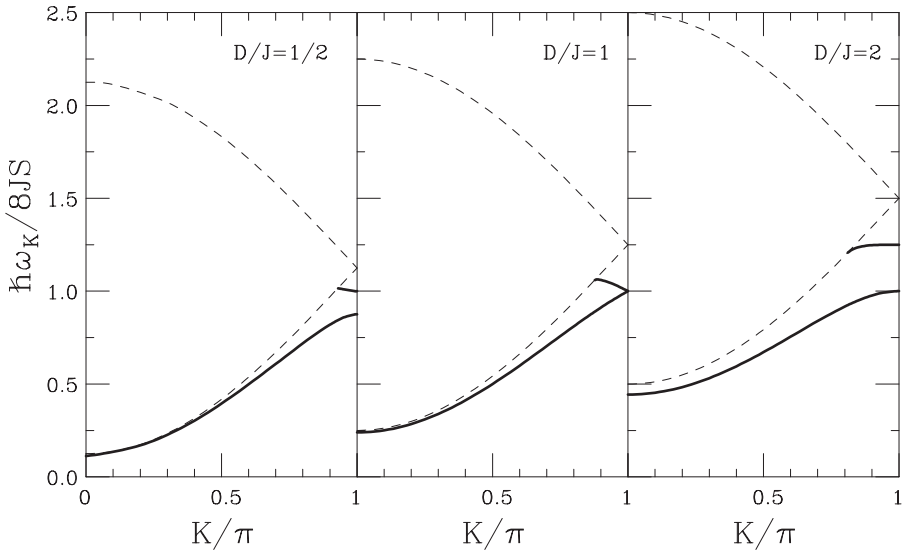

Fig. 5.5. Two-magnon bound state energy versus wavevector for the LC with $S = 1$ and several values of the single-ion anisotropy $D/J = 0.5$, 1 and 2. The light dashed lines represent the bottom and the top of the two-magnon band.

In the absence of exchange anisotropy ($J^{\perp} = J^{z} = J$), one bound state exists over the whole BZ and another bound state appears close to the zone boundary. The scenario for $S = 1$ and $D/J = 0.5, 1, 2$ is shown in Fig. 5.5. The wavevector K_c at which the second bound state occurs is given by $K_c/\pi = 0.93008$, 0.87766 and 0.81076 for $D/J = 0.5, 1$ and 2, respectively. The interval $K_c < K < \pi$ of wavevectors in which the second bound state exists increases as the single-ion anisotropy increases. In Tables 5.1–5.3, we give the numerical values of the energy eigenvalues of the bound states together with the associated probability of finding the two spin deviations on the same site for $D/J = 0.5$, 1 and 2, respectively. As one can see from Table 5.1, the bound state (1) existing over the whole BZ has a prevalent exchange character. Indeed, the associated probability of finding the two spin deviations on the same site is less than 1/3 for any K reaching its maximum at $K \simeq 0.8\pi$. On the contrary, the bound state (2) restricted to the region $0.93008\pi < K < \pi$ shows a prevalent single-ion character since $P_K^{(2)} \sim 1$ except when it is very near to K_c where the bound state enter the two-magnon band. An unexpected behaviour is seen in Table 5.2 for $D/J = 1$ where even at the ZB, where the two bound states are degenerate, the pure single-ion or exchange character does not occur. Both bound states are of prevalent single-ion character since they have a probability $P_{\pi}^{(1)}(0) = P_{\pi}^{(2)}(0) = 2/3$. Moving from $K = \pi$, both bound states maintain their prevalent single-ion character: The bound state (1) recovers the exchange nature for $K \lesssim 0.8\pi$. Note

Table 5.1. Two-spin wave bound states energy for $S = 1$ and $D/J = 0.5$.

K/π	$\frac{\hbar\omega^{(1)}}{8J}$	$P_K^{(1)}(0)$	$\frac{\hbar\omega^{(2)}}{8J}$	$P_K^{(2)}(0)$
0	0.12271	0.07592	—	—
0.1	0.13460	0.08230	—	—
0.2	0.16975	0.10102	—	—
0.3	0.22662	0.13080	—	—
0.4	0.30273	0.16960	—	—
0.5	0.39468	0.21447	—	—
0.6	0.49825	0.26123	—	—
0.7	0.60839	0.30273	—	—
0.8	0.71882	0.32219	—	—
0.9	0.81955	0.25774	—	—
0.93008	0.84453	0.19240	1.01539	0
0.95	0.85824	0.13020	1.01021	0.96141
0.99	0.87426	0.00773	1.00049	0.99805
1	0.875	0	1	1

Table 5.2. Two-spin wave bound states energy for $S = 1$ and $D/J = 1$.

K/π	$\frac{\hbar\omega^{(1)}}{8J}$	$P_K^{(1)}(0)$	$\frac{\hbar\omega^{(2)}}{8J}$	$P_K^{(2)}(0)$
0	0.23931	0.17961	—	—
0.1	0.25073	0.18636	—	—
0.2	0.28447	0.20628	—	—
0.3	0.33904	0.23843	—	—
0.4	0.41199	0.28137	—	—
0.5	1/2	1/3	—	—
0.6	0.59901	0.39244	—	—
0.7	0.70430	0.45686	—	—
0.8	0.81052	0.52500	—	—
0.87766	0.88983	0.57962	1.05902	0
0.9	0.91162	0.59552	1.06029	0.70869
0.95	0.95799	0.63123	1.03569	0.69970
0.99	0.99203	0.65965	1.00773	0.67361
1	1	2/3	1	2/3

that the expansions (5.5.26)–(5.5.29) for $D = J^{\perp} = J^z$ and $S = 1$ have to be replaced by

$$x_{\rm BS}^{(1)} = -\frac{1}{4}\left(1 + 2\cos\frac{K}{2} + 2\cos^2\frac{K}{2} - 3\cos^3\frac{K}{2} + \cdots\right), \qquad (5.5.35)$$

$$x_{\rm BS}^{(2)} = -\frac{1}{4}\left(1 - 2\cos\frac{K}{2} + 2\cos^2\frac{K}{2} + 3\cos^3\frac{K}{2} + \cdots\right), \qquad (5.5.36)$$

$$P_{K\to\pi}^{(1)}(0) = \frac{2}{3} - \frac{4}{9}\cos\frac{K}{2} - \frac{4}{27}\cos^2\frac{K}{2} + \frac{230}{81}\cos^3\frac{K}{2} + \cdots \qquad (5.5.37)$$

and

$$P_{K\to\pi}^{(2)}(0) = \frac{2}{3} + \frac{4}{9}\cos\frac{K}{2} - \frac{4}{27}\cos^2\frac{K}{2} - \frac{230}{81}\cos^3\frac{K}{2} + \cdots . \qquad (5.5.38)$$

Table 5.3. Two-spin wave bound states energy for $S = 1$ and $D/J = 2$.

K/π	$\frac{\hbar\omega^{(1)}}{8J}$	$P_K^{(1)}(0)$	$\frac{\hbar\omega^{(2)}}{8J}$	$P_K^{(2)}(0)$
0	0.44331	0.44074	—	—
0.1	0.45347	0.44795	—	—
0.2	0.48345	0.46941	—	—
0.3	0.53166	0.50458	—	—
0.4	0.59541	0.55279	—	—
0.5	0.67135	0.61337	—	—
0.6	0.75458	0.68596	—	—
0.7	0.83921	0.77038	—	—
0.8	0.91723	0.86479	—	—
0.81076	0.92479	0.87522	1.20711	0
0.85	0.95023	0.91270	1.23675	0.23507
0.9	0.97660	0.95618	1.24756	0.14936
0.95	0.99392	0.98805	1.24985	0.04583
0.99	0.99975	0.99951	1.25000	0.00197
1	1	1	1.25	0

From Table 5.3, we see that the bound state (1) existing over the whole BZ, has a prevalent single-ion character while the bound state (2) restricted to $0.81076\pi < K < \pi$ has a prevalent exchange character. This may be explained noticing that for large single-ion anisotropy ($D > J$), the lowest bound state becomes the single-ion one at zone boundary and it extends over the whole BZ.

The single-ion anisotropy also enters a new bound state in 2D and 3D. Numerical results were performed for a SC lattice[42,43] with $J^{\perp} = J^z = J$ and $S = 1$ along the high symmetry direction $\boldsymbol{K} = (K, K, K)$: a new "single-ion" bound state appears in addition to the three "exchange" bound states existing in the isotropic case (see the first panel of Fig. 5.4). For small anisotropy, let us say $D \lesssim J$, the four bound states exist in a restricted region close to the ZC. As the anisotropy increases, the "single-ion" bound state exists over a wider region of wavevectors extending towards $K = 0$. As for the 1D case, for a single-ion anisotropy $D > J$, the single-ion bound state is lower than the exchange bound state since at the ZC, the state with two deviations on the same site (single-ion bound state) has a lower energy: the energy cost of such a state with a spin reversal is only due to the exchange energy; indeed for $S = 1$, the anisotropy energy does not change when the spin is reversed since for $S_i^z = \pm 1$, one has $-D(S_i^z)^2 = -D$. The reduced dispersion of the spectrum observed for large anisotropy confirms that the excitation is of Ising-type. For very large anisotropy $D \sim 10 - 20J$, the single-ion bound state extends over the whole range $0 < K < \pi$. This peculiarity is the most striking discrepancy with respect to the isotropic case where the existence of bound states around the zone centre is prevented. For large uniaxial anisotropy, the "single-ion" bound state may become the lowest excitation crossing the single-spin wave energy spectrum. The occurrence of a bound state below the two-magnon band improves the chance of an experimental check.

In 2D, the bound states are evaluated for the TR lattice in the isotropic case[40] and for the anisotropic model[43] with $S = 1$, $D = 7.41J^z$, $J^{\perp} = 0.71J^z$, a choice of

parameters used to describe the actual compound $FeCl_2$, a triangular anisotropic ferromagnet in which the antiferromagnetic coupling between planes is an order of magnitude smaller than the ferromagnetic coupling in the triangular planes. The 2D case is qualitatively similar to the 1D case since at least one bound state exists for any wavevector. Results qualitatively similar to the SQ lattice shown in Fig. 5.2 are obtained in the TR isotropic ferromagnet.[40] The single-ion anisotropy enters one more bound state: The most important effect, however, is that the anisotropy splits the bound state existing over the whole BZ in the isotropic case, well below the two-magnon band with an increased chance of experimental check.

The study of the bound states has also been extended to the case of Heisenberg Hamiltonian with NNN interaction. In the case of a LC with NNN interaction,[44] the result is similar to that obtained in Section 5.2 until the NNN interaction becomes negative and large enough to change the ferromagnetic ground state into a non-collinear ground state.

Calculation of three-magnon bound states[45] have been performed in a SQ lattice with $S = 1/2$ for $\boldsymbol{K} = (K, K)$ for an isotropic and anisotropic Hamiltonian. The existence of four three-magnon bound states was proved in a region close to the ZC ($K \gtrsim 0.76\pi$).

An interesting question is about the experimental measure of the bound states. Since a direct measure of the bound state seems to be hopeless, one more direct approach seems to test the effect of the presence of the bound state on the one-magnon excitation that can be studied directly by means of the inelastic neutron scattering (INS). As we have seen in Section 4.5, Fig. 4.8, the presence of a bound state induces a sort of resonance in the magnon spectrum in proximity of the ZC. In particular, such a resonance occurs at a wavevector corresponding to the crossing of the simple spin wave energy spectrum with the damped bound state energy inside the two-magnon band.